Chemical Physics 35 (1978) 263–267

STUDY OF EXCITED FRAGMENT EMISSION FROM THE ELECTRON IMPACT DISSOCIATION OF VOLATILE MERCURY(II) HALIDES

J. ALLISON and R.N. ZARE
Department of Chemistry, Stanford University, Stanford, California 94305, USA

Received 10 August 1978

Emission resulting from collisions of 5–200 eV electrons with gaseous HgX_2 and CH_3HgX (X = Cl, Br, I) was characterized in the 3800–5600 Å region. HgX B–X emission dominates and absolute cross section as a function of electron energy were determined. The formation of electronically excited Hg atoms, and the trend of the cross sections with the nature of the halogen atom are discussed in terms of a simple charge transfer model.

1. Introduction

Recently laser action has been demonstrated for the B–X transitions of HgCl, HgBr, and HgI [1–7]. The excited HgX species have been produced by the photolysis of HgX_2, by high voltage discharges in HgX_2/rare gas mixtures, and by electron beam pumping of Hg/C X_4/rare gas mixtures. This study addresses the question of the role played by electron impact dissociation of HgX_2 and CH_3HgX in the generation of excited mercury monohalide fragments.

All the mercury monohalides have similar potential curves. The $X\,^2\Sigma^+$ ground state is weakly bound with a well depth of about 1 eV. It dissociates into ground state atoms. The first bound excited state, $B\,^2\Sigma^+$, is ionic, correlating with $Hg^+(^2S)$ and $Cl^-(^1S)$. This B state is more strongly bound than the X state but its internuclear equilibrium distance is much larger, causing the low vibrational levels of the B state to emit preferentially to the high vibrational levels of the X state (Franck–Condon principle). The latter appear to be rapidly relaxed so that population does not accumulate in the lower levels of the B–X laser transitions.

Emission from electron impact dissociation of the mercury dihalides (HgX_2) as well as the methyl mercury halides (CH_3HgX), where X = Cl, Br, I, were studied as a function of the electron energy. Absolute cross sections for the formation of excited HgX were determined.

2. Experimental

The experimental setup consists of two separately pumped chambers, one that houses the electron gun (thoriated tungsten emitter), the other that contains the target molecules. The gun chamber is evacuated by a 200 ℓ/s ion pump (Ultek); the target chamber is attached to a 800 ℓ/s 6″ diffusion pump (Varian). The electron beam (0–200 μA at 0–200 eV) passes through a rectangular slit (1 cm × 0.5 cm) that connects the two chambers. The compounds under study flow through the target chamber at a pressure of (1–2) × 10^{-4} torr; under these conditions the pressure in the gun chamber is about 5 × 10^{-6} torr. The emission perpendicular to the electron beam is focused onto a 1 m spectrometer (Interactive Technology) having a Centronic Q4283B S-20 photomultiplier cooled to –20°C. The slitwidths are 100–200 μ and the scan rates are 50–100 Å/min. Emission in the 3800–5600 Å region was recorded using a high speed picoammeter (Keithley).

The methyl mercury halides (Ventron Corp., Alpha Products) have sufficiently high pressure that they can be used without heating. The mercury dihalides (same vendor) required gently heating (10–20°C above room temperature). In addition, it was necessary to warm the target chamber to obtain the desired pressures. All pressures were measured using a Bayard–Alpert ionization gauge. The pressure

readings were corrected for the response of the different gases using the procedure of Holanda [8].

Absolute cross sections were calculated using the known hydrogen Balmer emission cross sections from electron impact dissociation of CH_4. In particular, we use as a reference the cross section of (6.56 ± 0.33) × 10^{-19} cm^2 for the formation of H^* emission at 4861 Å by 100 eV electrons [9].

3. Results

The cross sections we report refer to specific emission wavelengths. For the HgX B–X emission, the cross sections were calculated for the most intense transition, usually corresponding to the (2,2,0) band. In each case, the cross sections are normalized to constant electron flux. As a first step, we recorded emission spectra resulting from the electron bombardment of CH_3HgX and HgX_2 using 5–200 eV electrons. A number of generalizations can be made: (1) in all cases, HgX B–X emission occurs; (2) emission from highly excited Hg atoms have the greatest peak height while emission from the HgX^* molecules have the greatest integrated intensity; (3) the relative emission intensities from Hg 7 $^1S_0$, 6 $^1D_2$, and 7 $^3S_1$, change at low electron energies, but are constant at energies above 60 eV, where emission from Hg 7 $^3S_1$ dominates; (4) cross sections for Hg^* emission increase with electron energy more rapidly than for HgX^*; (5) HgX^* emission increases in going from Cl to I for both CH_3HgX and HgX_2; (6) no X^* emission or ionic emission is observed in the spectral region studied; (7) in CH_3HgX, CH(A–X) and H^* emission appears at higher energies; (8) the vibrational distribution of the molecular emission does not depend on electron energy; and (9) the vibrational distribution in HgX^* is broader from HgX_2 than CH_3HgX.

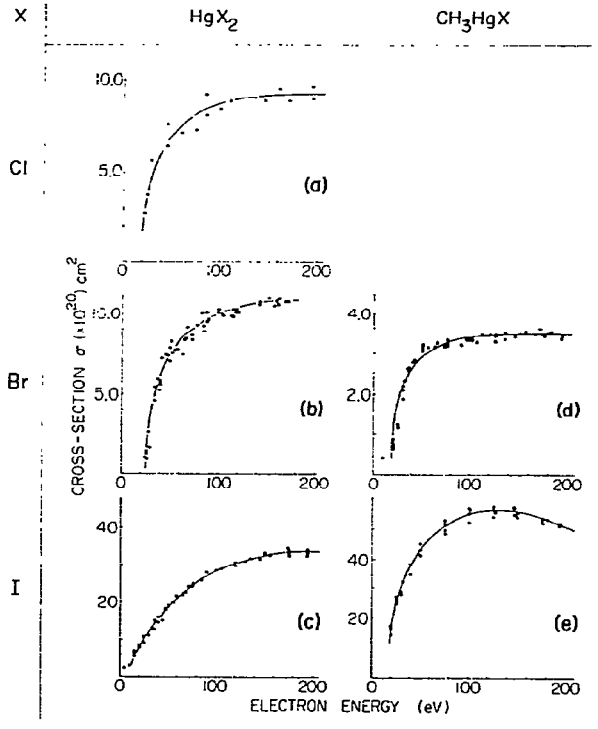

Fig. 1. Cross sections for HgX B–X emission at the wavelength λ_{max} as a function of incident electron energy: (a) λ_{max} = 5576 Å; (b) λ_{max} = 5018 Å; (c) λ_{max} = 4412 Å; (d) λ_{max} = 5018 Å and (e) λ_{max} = 4412 Å.

Fig. 1 shows the energy dependence of HgX^* emission for the compounds studied. Relative cross sections were converted into absolute values by referencing the observed emission at 100 eV to that for the production of the Balmer β line from methane at the same electron energy. Table 1 lists the values of the absolute cross sections at 100 eV. The error

Table 1
Cross sections for emission at λ_{max} for 100 eV electrons (values × 10^{20} cm^2)

	X = Cl	X = Br	X = I
HgX_2	8.74 ± 1.05	9.68 ± 1.34	28.4 ± 3.2
CH_3HgX	1.08 ± 0.43	3.35 ± 0.14	55.6 ± 1.1
λ_{max}	5576 Å	5018 Å	4412 Å
IP(CH_3HgX)–EA(X)	7.3 eV	6.8 eV	6.2 eV
IP(HgX_2)–EA(X)	7.8 eV	7.2 eV	6.5 eV

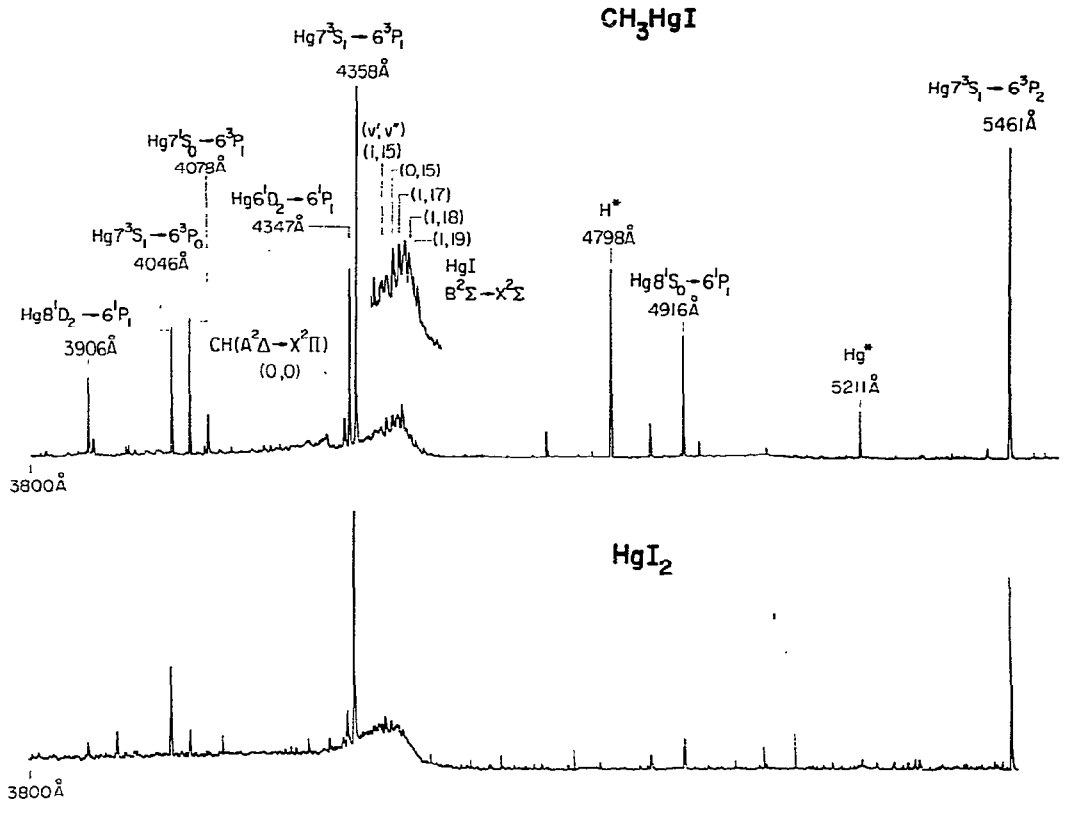

Fig. 2. Emission spectra for 100 eV electrons incident on CH_3HgI and HgI_2 in the 3800–5600 Å region.

estimates represent only the statistical uncertainty in the measurements. The largest systematic error is expected to be the pressure measurement. We estimate that the absolute cross sections in table 1 are accurate to about 20%.

In the region of HgCl B–X emission, background emission from the electron gun begins to appear. This was corrected for in cross section calculations for $HgCl_2$, but the signal was too weak for CH_3HgCl to determine the energy dependence of the formation of HgCl*. However, the cross section at 100 eV was determined.

Fig. 2 presents the emission spectrum (3800–5600 Å) for 100 eV electrons incident on HgI_2 and CH_3HgI. The results are characteristic of the comparison between emission from HgX_2 and CH_3HgX. Although the peak intensity of the Hg $7\,^3S_1 \rightarrow 6\,^3P_1$ atomic transition greatly exceeds the peak intensity of the HgI B–X emission, the integrated intensity of the latter is larger. Note that the molecular emission from HgI_2 is broader than from CH_3HgI.

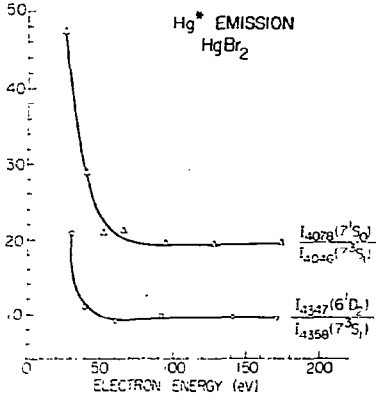

Fig. 3. Intensity ratios of selected atomic mercury transitions from $HgBr_2$ as a function of electron energy.

In the methyl mercury halides we see evidence that these compounds decompose to a small extent on the walls of the apparatus to form Hg and CH_3X. This is indicated by Hg($8\ ^1D_2$) emission at 3906 Å formed by electron impact on Hg, but not on the parent molecule.

Fig. 3 illustrates the variation in atomic mercury emission over the 3800–5600 Å spectral region as a function of electron impact energy. The results are taken from electron impact on $HgBr_2$, but are typical of the other molecules studied. As the electron energy increases, the intensity ratio of different atomic transitions approaches a constant value. Population of the Hg $7\ ^3S_1$ level dominates.

The variation with electron energy of the HgX emission relative to the most intense mercury emission is shown in fig. 4 for $HgBr_2$ and CH_3HgBr. It is to be emphasized that the ratios refer to peak heights. If instead, we compare integrated intensities, then it is clear that the molecular emission is stronger, and at the lower electron energies (25 eV) is an order of magnitude brighter than the atomic emission. A search was made at still lower electron energies (to ~ 10 eV) for enhanced molecular emission, but for all the compounds studied, no such effect was found.

Figs. 5 and 6 present the energy dependence of H^* emission in CH_3HgI and CH^* emission in CH_3HgBr. Again, the behavior is representative of the other compounds studied. As the electron energy increases, emission from both of these species also increases relative to mercury emission.

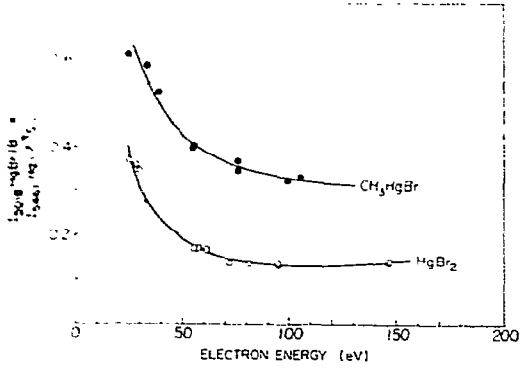

Fig. 4. Comparison of molecular to atomic peak intensities as a function of electron energy for the fragmentation of CH_3HgBr and $HgBr_2$.

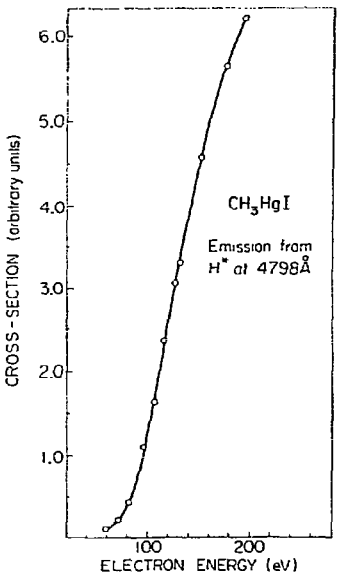

Fig. 5. Excited H atom emission from CH_3HgI as a function of electron impact energy.

4. Discussion

The present studies have much in common with the previous investigations of electron impact excitation of molecules. We find that at low electron energies, electron exchange processes are important, causing the production of excited fragments with different spin multiplicities. As fig. 3 shows, the most intense emission from excited triplet states of mercury occurs at lower electron energies. We also find that the vibrational structure of the molecular emission

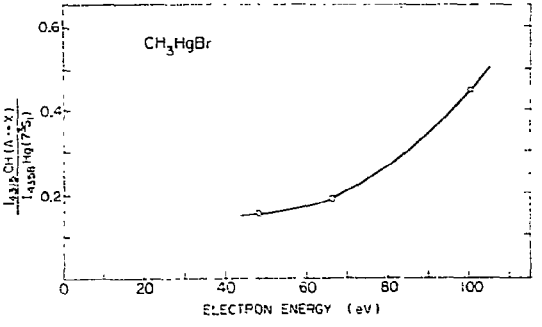

Fig. 6. Intensity ratio of CH(A–X) emission to Hg $7\ ^3S_1$–$6\ ^3P_1$ emission from CH_3HgBr as a function of electron impact energy.

in both CH and HgX is not energy dependent, in agreement with electron impact studies on CH_4, C_2H_4 and C_2H_2 which also show the same behavior for CH emission [9].

We do, however, find broader emission from HgX in HgX_2 than CH_3HgX. This agrees with previous photodissociation studies of the same compounds [10]. We also note that photodissociation of HgX_2 by an argon fluoride laser at 193 nm results in excited mercury emission [11]. In particular, emission almost exclusively from the Hg $7\,^3S_1$ level. Again, this is in agreement with the present electron impact studies.

The central problem in electron impact excitation of molecules is to understand why certain pathways for the production of excited fragments occur preferentially. In what follows, we present a simple molecular orbital picture to explain: (1) the predominance of HgX emission, (2) the increase of the cross section for HgX emission in going from Cl to I for HgX_2 and for CH_3HgX, and (3) the emission from Hg^* but not X^* in the spectral region studied.

Let us consider the change in bonding upon electron impact excitation of CH_3HgX. In its ground state, the two valence electrons on Hg may be described to good approximation as covalently bonded, one being shared with the electron in the sp^3 orbital of CH_3, the other shared with the electron in the sp orbital on X. Upon excitation, the electronic distribution in CH_3HgX is transferred to the more ionic $CH_3Hg^+X^-$ corresponding to the transfer of the shared electron between Hg and X to the filling of the p hole on X (see fig. 7). This leads to a strongly allowed parallel charge transfer band system. The excess energy induces fragmentation of the CH_3–Hg bond, leaving HgX in the (ionic) B state. An analogous molecular orbital argument can be made for the electron impact excitation of HgX_2.

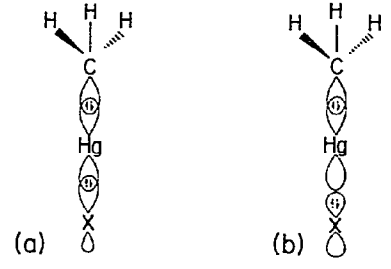

Fig. 7. Rearrangement of valence electrons when the covalently bound CH_3HgX molecule shown in (a) make a transition to the ionic charge transfer state $CH_3Hg^+X^-$ shown in (b).

A rough estimate of the energy required to produce $CH_3Hg^+X^-$ or XHg^+X^- is given by the ionization potential of the parent molecule, IP(P), minus the electron affinity of the halogen atom, EA(X). Table 1 lists these differences and shows that the cross section for HgX emission increases with decreasing values of IP(P)–EA(X). Moreover, this extremely simple model (fig. 7) provides a rationale why Hg^* emission is observed but not X^* emission. The Hg^* emission can be crudely pictured as occurring from the recombination of Hg^+ with the electron on X^-.

From the standpoint of potential laser applications, the present study suggests that, due to the small size of the cross sections, the direct formation of HgX^* from electron impact excitation of HgX_2 is not the major pathway for laser systems using discharges in or e-beam pumping of the parent molecule.

This work is supported in part by the Office of Naval Research under N 00014-78-C-0457 and the Air Force Office of Scientific Research under AFOSR 77-3363. One of us (J.A.) thanks the National Science Foundation for a National Needs Postdoctoral Fellowship.

References

[1] J.H. Parks, Appl. Phys. Letters 31 (1977) 192.
[2] J.H. Parks, Appl. Phys. Letters 31 (1977) 297.
[3] J.G. Eden, Appl. Phys. Letters 31 (1977) 448.
[4] W.T. Whitney, Appl. Phys. Letters 32 (1978) 239.
[5] E.J. Schimitschek, J.E. Celto and J.A. Trias, Appl. Phys. Letters 31 (1977) 608.
[6] E.J. Schimitschek and J.E. Celto, Opt. Letters 2 (1978) 64.
[7] K. Tang and D. Huestis, Appl. Phys. Letters 32 (1978) 276.
[8] R. Holanda, J. Vacc. Sci. Tech. 10 (1973) 1133.
[9] C.I.M. Beenakker, Ph.D. Thesis, State University of Leyden, The Netherlands (1971).
[10] A. Terenin and N. Prileshajeva, Acta. Phys. URSS 1 (1935) 768.
[11] T.A. Cool, J.A. Mc Gavrey and A.C. Erlandson, Chem. Phys. Letters 58 (1978) 108.